Intrinsic Viscosity of Oligo- and Polyisobutylenes. Treatments of Negative Intrinsic Viscosities

Fumiaki Abe, Yoshiyuki Einaga, and Hiromi Yamakawa*

Department of Polymer Chemistry, Kyoto University, Kyoto 606, Japan

Received January 2, 1991; Revised Manuscript Received March 20, 1991

ABSTRACT: The intrinsic viscosity, $[\eta]$, was determined for 19 samples of oligo- and polyisobutylenes (PIB) in the weight-average molecular weight, M_w, range from 1.12×10^2 to 1.79×10^6 in isoamyl isovalerate (IAIV) at 25.0 °C (Θ) and in benzene at 25.0 °C (Θ). Double-logarithmic plots of $[\eta]$ against M_w for PIB in the two Θ solvents follow the same asymptotic straight line of slope $^1/_2$ for $M_w > 10^5$. The plot deviates upward slightly from this straight line with decreasing M_w for $6 \times 10^2 \lesssim M_w \lesssim 10^4$ in IAIV but deviates downward rather appreciably for $6 \times 10^2 \lesssim M_w \lesssim 10^5$ in benzene. In this range of M_w, the values of $[\eta]$ are definitely larger in IAIV than in benzene, with the difference being almost independent of M_w. However, as M_w and, hence, $[\eta]$ are further decreased, the difference becomes small, then the relation reverses at M_w corresponding to the trimer or so, and finally $[\eta]$ becomes negative in both solvents. The negative intrinsic viscosity may be regarded as arising from specific interactions between solute and solvent molecules such that a liquid structure of some kind existing in the solvent is destroyed in the vicinity of a solute molecule. Such effects cannot be treated within the framework of classical hydrodynamics. Thus, an attempt is made to remove them, though empirically, in order to analyze the present data by the use of the hydrodynamic theory of $[\eta]$ of the helical wormlike touched-bead model. The results show that the PIB chain is very thin and flexible, taking the local conformation close to the 8_3 helix in dilute solutions.

Introduction

In this series of experimental papers on dilute-solution properties of oligomers and polymers, we have already presented some data for the mean-square optical anisotropy, $\langle\Gamma^2\rangle$, intrinsic viscosity, $[\eta]$, mean-square radius of gyration, $\langle S^2\rangle$, and scattering function, $P_s(k)$, for atactic polystyrene (a-PS)[1-4] and also for $\langle S^2\rangle$ and $[\eta]$ for atactic poly(methyl methacrylate) (a-PMMA)[5,6] and have analyzed the data at the Θ temperatures on the basis of the helical wormlike (HW) chain model[7,8] to obtain information about the local chain conformations. Since these polymers are asymmetric ones, we expended great care in preparing well-characterized samples of fixed stereochemical composition as well as of narrow molecular weight distribution. The samples used have the fractions of racemic diads $f_r = 0.59$ for a-PS[1,9] and 0.79 for a-PMMA[10] independent of molecular weight, with the distributions of diads obeying Bernoullian statistics.

In the present and forthcoming papers, we thus proceed to make a similar study of symmetric polymers, for which the stereochemical composition need not be considered. The present paper deals with $[\eta]$ of polyisobutylene (PIB), a typical symmetric polymer, in Θ solvents. For this polymer, especially for the oligomers, much care should, however, be given to the regulation of the structures of end groups.

Now the data obtained long ago by Fox and Flory[11] for PIB in benzene at 25.0 °C (Θ) show that the double-logarithmic plot of $[\eta]$ against the molecular weight, M, follows a straight line of slope $^1/_2$ over a wide range of M greater than 530. This is in contrast to the cases of a-PS[2] and a-PMMA[6] for which the plot exhibits remarkable inflection with a slope smaller than $^1/_2$ in the range of small or intermediate M. In the present case, therefore, it is clear that it is impossible to determine all the HW model parameters from an analysis of data for $[\eta]$ alone. For this purpose, we must then obtain data for another property, e.g., $\langle S^2\rangle$, from small-angle X-ray scattering measurements over a wide range of M. However, the measurements could not be carried out since none of the available Θ solvents for PIB yield ample excess electron density. Thus, we attempt to analyze data for $[\eta]$ assuming the local chain conformation in solution on the basis of the crystallographic data, thereby assigning proper values to two of the HW model parameters. Specifically, we assume the Kratky–Porod (KP) wormlike model[12] as a special case of the HW chain. The adequacy of this assumption may be judged from the values of the other parameters determined.

In practice, we carried out measurements of $[\eta]$ over a wide range of M, including the dimer, choosing benzene and isoamyl isovalerate (IAIV) as Θ solvents. In anticipation of the results, it is very important to note that $[\eta]$ of the few lowest oligomers becomes negative in these Θ solvents. The fact that $[\eta]$ becomes negative is already known for certain oligomers, e.g., *n*-alkanes in benzene[13] and butadiene oligomers in Aroclor 1248 and/or 1254.[14] In fact, the negative $[\eta]$ was discovered a long time ago for a variety of binary simple liquid mixtures, e.g., for benzene in ethanol (at 25 °C)[15] and carbon tetrachloride in tetrachloroethylene (at 25 °C).[16] It means a decrease in the solution viscosity below that of the solvent by addition of a solute, and this may be regarded as arising from specific interactions between solute and solvent molecules such that a liquid structure of some kind existing in the solvent is destroyed in the vicinity of a solute molecule.

Now all polymer transport theories have been developed so far within the framework of classical hydrodynamics, which cannot treat such effects of specific interactions on $[\eta]$, giving necessarily the positive Einstein intrinsic viscosity of a sphere (polymer bead). Thus, we must remove the contributions of specific interactions from the raw data for $[\eta]$ so that the corrected $[\eta]$ may be at least positive for all possible M to be fit for an analysis by the use of our transport theory of $[\eta]$ of the HW touched-bead model.[17] This is one of the important problems in the present paper.

Experimental Section

Materials. Of the PIB samples used in this work, those with weight-average molecular weights, M_w, larger than 5×10^3 are fractions from the commercial samples of Enjay Chemical Co., named Vistanex LM-MS, L-80, and L-200. The PIB chain in

0024-9297/91/2224-4423$02.50/0

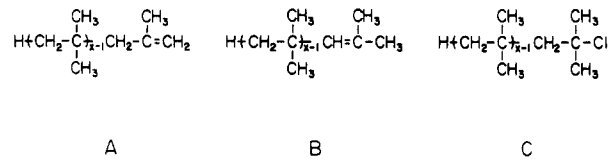

A B C

Figure 1. Chemical structures of the PIB chains with different end groups. A and B, both contained in the samples prepared by cationic polymerization and also the products obtained by dehydrochlorination of the samples C prepared by living cationic polymerization (see the text).

those original samples as prepared by cationic polymerization has a hydrogen atom at one end and a 2-methylprop-2-enyl (type A) or 2-methylprop-1-enyl (type B) group at the other,[18] as shown in Figure 1. For such large M_w, there is no disorder in the sequence such as branching and dislocation of the methyl side groups and the double bond, while this may possibly occur in the oligomers prepared by cationic polymerization.[18]

The oligomer samples with $5 \times 10^2 < M_w < 5 \times 10^3$ were therefore obtained from two original samples with different M_w, which are designated OIBII and OIBIII, prepared by living cationic polymerization by the courtesy of Dr. Y. Hirokawa of Nippon Zeon Co. In these, there is no disorder in the chain sequence, but the chain has a tertiary chloro (type C) group at one end, as shown in Figure 1. Thus, we removed this terminal chlorine atom by dehydrochlorination following the procedure of Kennedy et al.[19] so that we may have almost the same structures of end groups as the above commercial samples prepared by cationic polymerization. These structures were examined by ^{1}H NMR spectroscopy. The spectra were recorded on a JEOL JNM GX-400 spectrometer at 399.7 MHz in chloroform-*d* containing tetramethylsilane as an internal standard with a sample concentration of 0.5 wt % at 24.0 °C. The measurements were carried out with a radio-frequency pulse angle of 45° and a pulse repetition time of 15 s, which is about 5 times as long as the longest spin–lattice relaxation time of the nuclides under investigation. In anticipation of the results, we note that the dehydrochlorination proceeded completely and that 96% of the PIB chains in the products both from OIBII and OIBIII, which are designated OIBII$_1$ and OIBIII$_1$, respectively, are of type A and the remaining 4% are of type B. We also note that it was very difficult to achieve complete hydrogenation of these samples as well as the commercial ones, and therefore, it was given up.

Samples OIBII$_1$ and OIBIII$_1$ were separated into fractions of narrow molecular weight distribution by preparative gel permeation chromatography (GPC) with two serially connected Tosoh G2000H$_6$ (600 × 50 mm) columns using chloroform as an eluent. The Vistanex PIB samples were fractionated by fractional precipitation using benzene as a solvent and methanol as a precipitant. In each case, the fractionation was repeated several times. The main fractions finally obtained were dried under reduced pressure at 40–60 °C from their benzene or chloroform solutions for $M_w < 2 \times 10^4$ and freeze-dried from their cyclohexane solutions for $M_w > 2 \times 10^4$ after filtration through a Teflon membrane of pore size 0.10–0.45 μm. The ratio of M_w to the number-average molecular weight, M_n, was determined by analytical GPC.

In addition to the above samples, the x-mer samples (x = 2–4), which are designated OIBx, were also investigated in this work. The compounds having the type A and B structures with $x = 2$ are commercially available as 2,4,4-trimethyl-1-pentene (TM1P) (Aldrich Chemical Co., purity > 99%) and 2,4,4-trimethyl-2-pentene (TM2P) (Aldrich, purity > 98%), respectively. Thus, the dimer sample OIB2 was prepared by mixing TM1P and TM2P in the ratio 96:4 to be consistent with the above NMR results for the OIBII$_1$ and OIBIII$_1$ samples. The trimer sample OIB3 was obtained from the commercial triisobutylene (Nacalai Tesque Inc.) by distillation under reduced pressure and was found from ^{1}H NMR to contain 4,4-dimethyl-2-neopentyl-1-pentene (60%) and 2,2,4,6,6-pentamethyl-3-heptene (40%). As for the tetramer sample OIB4, the commercial tetraisobutylene (Tokyo Kasei Kogyo Co., purity > 98%) was used as delivered. From ^{1}H NMR, it was found to contain many structural isomers. Thus, samples OIB3 and OIB4 are not strictly consistent with the others in the chemical structure.

The solvent IAIV (Tokyo Kasei Kogyo Co.) used for viscosity and light-scattering (LS) measurements was purified by distillation under reduced pressure after dehydration with potassium carboxide. The other solvents, benzene and *n*-heptane, used for viscosity and LS measurements, respectively, were purified according to standard procedures. The solvent chloroform-*d* used for NMR measurements was of reagent grade.

Light Scattering. LS measurements were carried out to determine M_w of the samples with $M_w > 10^3$ and also the Θ temperature of IAIV solutions. The values of M_w were determined for all those samples in *n*-heptane at 25.0 °C and for some of them with $M_w > 4 \times 10^5$ also in IAIV at Θ. For the determination of Θ, the second virial coefficient A_2 was measured for three samples at several temperatures ranging from 20 to 40 °C.

A Fica 50 light-scattering photometer was used for all the measurements with vertically polarized incident light of wavelength 436 nm. For calibration of the apparatus, the intensity of light scattered from pure benzene was measured at 25.0 °C at a scattering angle 90°, where the Rayleigh ratio $R_{U_u}(90°)$ of pure benzene was taken as 46.5×10^{-6} cm^{-1}. The depolarization ratio, ρ_u, of pure benzene at 25.0 °C was determined to be 0.41 ● 0.01 by the method of Rubingh and Yu.[20] Scattering intensities were measured at four or five different concentrations and at scattering angles ranging from 30 to 150° except for a few samples with very high M_w, for which measurements were performed also at a scattering angle of 22.5°. The obtained data were analyzed by the Berry square-root plot.[21] In the present case, corrections for the optical anisotropy were unnecessary since the degree of depolarization was found to almost vanish even for the lowest molecular weight sample in *n*-heptane.

As shown in the Results section, the Θ temperature of the IAIV solutions is 25.0 °C, while *n*-heptane is a good solvent for PIB. Thus, the most concentrated solution of each sample in IAIV was prepared by continuous stirring at ca. 50 °C for 3–4 days. (Complete dissolution of PIB in IAIV was confirmed from the flow times.) The most concentrated *n*-heptane solution was prepared by continuous stirring at 20–50 °C for 1–3 days, depending on M_w. The most concentrated solutions were optically purified by filtration through a Teflon membrane of pore size 0.10–0.45 μm. (From the flow times, the filtration was confirmed to cause neither a change in polymer concentration nor chain scission.) The solutions of lower concentrations were obtained by successive dilution. The mass concentrations, c, were calculated with the densities of the solvents.

The refractive index increment, $\partial n/\partial c$, was measured at 436 nm for PIB samples with low to high M_w in *n*-heptane at 25.0 °C and for one sample with high M_w (=4.22×10^5) in IAIV at 25.0 °C by the use of a Shimadzu differential refractometer. For the *n*-heptane solutions, $\partial n/\partial c$ increased from 0.134_5 to 0.143_5 cm^3/g as M_w was increased from 1.01×10^3 to 8.73×10^3, and it remained constant for higher M_w. The value in IAIV was 0.110_3 cm^3/g. (We note that $\partial n/\partial c \simeq 0$ in benzene.)

Viscosity. Viscosity measurements were carried out for all the samples in benzene at 25.0 °C (Θ) and in IAIV at 25.0 °C (Θ). We note that the former Θ temperature was determined by Krigbaum and Flory[22] from critical solution temperatures. We used two conventional viscometers of the Ubbelohde type and also two (four-bulb) spiral capillary viscometers of the same type as used previously.[2,6] We then determined the specific viscosity, η_{sp}, rather accurately in the ranges from 0.001 to 0.6 for $[\eta] > 0$ and from −0.01 to −0.007 for $[\eta] < 0$, keeping the difference between flow times of the solution and solvent greater than 10 s except for OIB3 in IAIV. The flow time was measured to a precision of 0.1 s, and the test solutions were maintained at constant temperature within ±0.005 °C during the measurements. In the measurements for IAIV solutions of PIB with $M_w > 1.5 \times 10^6$, the surface of the water in a thermostat was covered with liquid paraffin to remove the possible effects of moisture. Without this protection, the flow time of the solution became shorter as time elapsed, probably because of the hygroscopic property of IAIV.

The test solutions were prepared in the same manner as in the case of LS measurements except for the solutions of the three lowest molecular weight samples, OIB2, OIB3, and OIB4. Since they are volatile liquids, each was mixed with benzene or IAIV, followed by stirring for ca. 1 h, just before measurement.

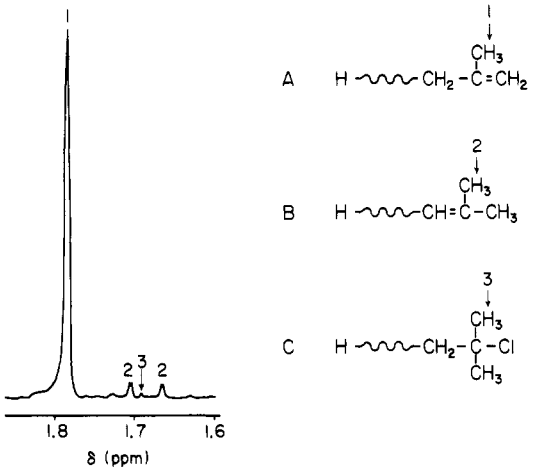

Figure 2. Part of the ^1H NMR spectrum of the product $OIBII_1$ obtained by dehydrochlorination. The attached numbers identify its absorption peaks with the methyl protons in the three types of end groups indicated.

Density corrections were not made for both benzene and IAIV solutions of the samples with $M_w > 790$, since the solution and solvent had the same density independent of c within experimental error. However, corrections were made in the calculations of c and also of the relative viscosity, η_r, for the solutions of OIB2, OIB3, OIB4, and OIB11. The solution density was measured with a pycnometer of the Lipkin–Davison type.

The obtained data for η_{sp} and η_r were treated as usual by the Huggins and Fuoss–Mead plots to determine $[\eta]$ and the Huggins coefficient, k'.

Results

Dehydrochlorination. Products $OIBII_1$ and $OIBIII_1$ obtained by dehydrochlorination of the respective original samples prepared by living cationic polymerization may possibly contain PIB chains having end groups of the three types, A, B, and C, shown in Figure 1. A quantitative analysis of these groups was made by ^1H NMR spectroscopy. Figure 2 shows a part of the spectrum for $OIBII_1$ including absorption peaks due to the methyl protons in the end groups indicated, the attached numbers identifying the former with the latter. The assignments of peaks 1 and 3 were made on the basis of the results obtained by Kennedy et al.[19] and Kaszas et al.,[23] respectively, for similar PIB samples in carbon tetrachloride. On the other hand, peaks 2 were assigned on the basis of the present result obtained for the type B dimer, TM2P, under the same condition, where full assignments were possible. From the relative intensities of the peaks in Figure 2, it was found that the product, $OIBII_1$, contains only a negligibly small amount of type C (unreacted) and that 96% is of type A and the remaining 4% is of type B. We note that Kennedy et al.[19] have obtained the result that their dehydrochlorination product contains only type A chains. This may be due to the poor resolving power of their 60 MHz spectrometer.

We also examined the whole sample $OIBIII_1$ and the fraction OIB14 (with $M_w = 792$) from $OIBII_1$ and obtained the same analytical result as above. Thus, the compositions of all the final samples from $OIBII_1$ and $OIBIII_1$ may be regarded as the same, independent of M_w.

Molecular Weights and Their Distributions. The values of M_w and M_w/M_n for all the samples used in this work are given in Table I, where samples OIB11–OIB26 are from $OIBII_1$ and sample OIB32 from $OIBIII_1$. (The value of M_w/M_n for sample PIB180 could not be determined for lack of the GPC calibration curve in the necessary range.) Of those, samples OIB2, OIB3, and OIB4 may be assumed to be completely monodisperse as indicated, so that their M_w's were calculated from their chemical formulas. The values of M_w for OIB11 and OIB14 were determined by analytical GPC with a calibration curve of M_w vs elution time obtained from elution peaks for the samples with known M_w. The other values of M_w were determined from LS measurements in n-heptane, the figures in parentheses in the table representing the values in IAIV, as mentioned in the Experimental Section. The molecular weight distributions of the samples may be regarded as sufficiently narrow except for that of sample PIB120.

Table I
Values of M_w and M_w/M_n for Oligo- and Polyisobutylenes

sample	M_w	M_w/M_n
OIB2	1.12×10^2	1.00
OIB3	1.68×10^2	1.00
OIB4	2.24×10^2	1.00
OIB11	6.41×10^2	1.01
OIB14	7.92×10^2	1.01
OIB18[a]	1.01×10^3	1.02
OIB22	1.25×10^3	1.02
OIB26	1.47×10^3	1.02
OIB32	1.81×10^3	1.04
PIB1	8.73×10^3	1.10
PIB2	1.66×10^4	1.08
PIB3	2.79×10^4	1.07
PIB5	4.85×10^4	1.06
PIB9	8.55×10^4	1.08
PIB13	1.30×10^5	1.09
PIB40	4.19×10^5 (4.22×10^5)[b]	1.09
PIB80	8.54×10^5 (8.19×10^5)	1.09
PIB120	1.21×10^6 (1.18×10^6)	1.16
PIB180	1.79×10^6 (1.76×10^6)	

[a] M_w's of OIB18–PIB180 were determined from LS measurements in n-heptane. [b] The figures in parentheses represent the values in IAIV.

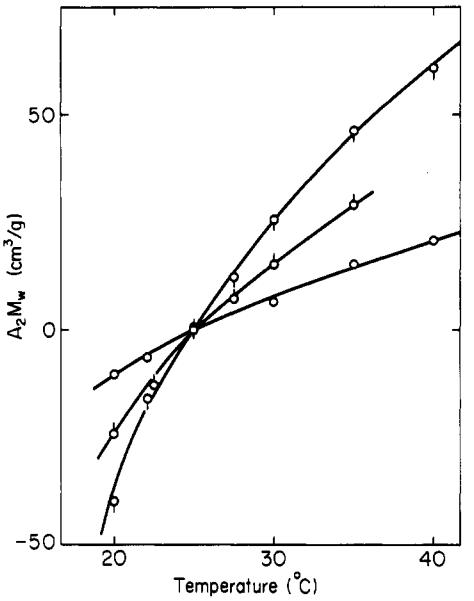

Figure 3. Plots of A_2M_w against temperature for PIB samples in IAIV. (○) PIB40; (◇) PIB80; (▽) PIB120.

θ Temperature. Figure 3 shows plots of A_2M_w against temperature for the three samples, PIB40, PIB80, and PIB120, in IAIV. It is seen that A_2 vanishes at the same temperature independent of M_w, leading to the conclusion that the θ temperature is 25.0 °C for IAIV solutions of PIB. This value of θ is larger by ca. 3 °C than the value obtained by Matsumoto et al.[24] for fractions from the same Vistanex PIB samples as used in this work. The decrease in θ in the latter may be in part due to the possible contamination of the solvent IAIV with its isomers. (Our solvent was examined by gas chromatography and found to contain no impurities.)

Table II
Results of Viscometry on Oligo- and Polyisobutylenes in IAIV at 25.0 °C and in Benzene at 25.0 °C

	IAIV (25.0 °C)		benzene (25.0 °C)	
sample	$[\eta]$, dL/g	k'	$[\eta]$, dL/g	k'
OIB2	−0.0145		−0.0072	
OIB3	−0.0024		0.0005	
OIB4	0.0071		0.0058	
OIB11	0.0301	0.77	0.0229	0.92
OIB14	0.0338	0.73	0.0259	0.83
OIB18	0.0369	0.65	0.0292	0.65
OIB22	0.0410	0.59	0.0328	0.70
OIB26	0.0439	0.59	0.0363	0.68
OIB32	0.0482	0.69	0.0400	0.63
PIB1	0.108	0.51	0.0986	0.67
PIB2	0.141	0.55	0.133	0.56
PIB3	0.180	0.51	0.176	0.52
PIB5	0.241	0.52	0.229	0.50
PIB9	0.318	0.46	0.307	0.54
PIB13	0.396	0.50	0.391	0.56
PIB40	0.709	0.56	0.715	0.65
PIB80	0.998	0.60	1.01	0.71
PIB120	1.17	0.50	1.20	0.73
PIB180	1.46	0.73	1.46	0.78

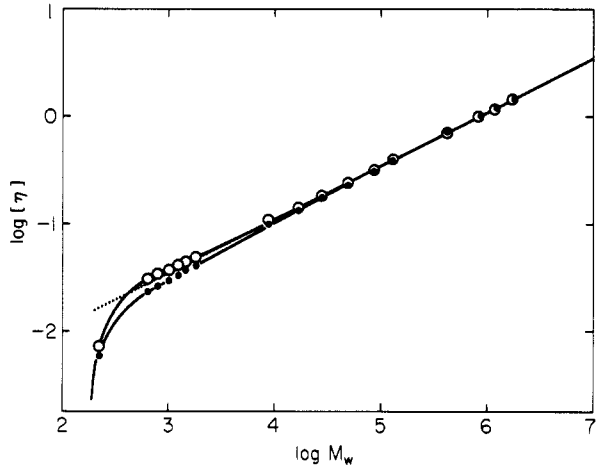

Figure 4. Double-logarithmic plots of $[\eta]$ (in dL/g) against M_w for PIB. (○) In IAIV at 25.0 °C; (●) in benzene at 25.0 °C. The dotted straight line has a slope of 0.5.

Viscosity. Intrinsic viscosity data for all the PIB samples in the two Θ solvents are summarized in Table II along with the values of the Huggins coefficient, k'. The latter values for OIB2, OIB3, and OIB4 are omitted from the table since k' becomes extraordinarily large for vanishingly small $[\eta]$ even if the Huggins plot itself has a finite, normal slope. It is very important to see that $[\eta]$ is negative for OIB2 both in IAIV and in benzene and for OIB3 in IAIV, and small positive for OIB3 in benzene. The values of $[\eta]$ for the two components, TM1P and TM2P, of OIB2 are given in Table III. The difference between them is ca. 10% in any of the two solvents, indicating that the structures of the end groups have rather appreciable influences on $[\eta]$. Note that the values of $[\eta]$ for OIB2 in IAIV and in benzene are close to the respective weight averages of $[\eta]$ for TM1P and TM2P.

Figure 4 shows double-logarithmic plots of $[\eta]$ (in dL/g) against M_w for the data, except for OIB2 and OIB3, in IAIV (unfilled circles) and in benzene (filled circles), both at 25.0 °C (Θ). The solid curves connect the data points smoothly, and the dotted line indicates a common asymptotic straight line of slope $^1/_2$ for the two sets of data, which agree with each other for $M_w > 10^5$. This agreement implies that the unperturbed dimensions, $\langle S^2 \rangle$ (and also the Flory–Fox factors Φ), of PIB in these two Θ solvents are the same in the random coil limit. It is also seen that the plot deviates upward slightly from the dotted straight line with decreasing M_w for $6 \times 10^2 \lesssim M_w \lesssim 10^4$ in IAIV but deviates downward rather appreciably for $6 \times 10^2 \lesssim M_w \lesssim 10^5$ in benzene. The latter behavior is in contrast to the cases of a-PS[2] and a-PMMA,[6] for which appreciable upward deviation occurs. More remarkable is the fact that the data points (lowest) for OIB4 in both solvents drop to a great extent.

Table III
Intrinsic Viscosities of the Isobutylene Dimers with Different End Groups in IAIV at 25.0 °C and in Benzene at 25.0 °C

	$[\eta]$, dL/g			$[\eta]$, dL/g	
	IAIV	benzene		IAIV	benzene
sample	(25.0 °C)	(25.0 °C)	sample	(25.0 °C)	(25.0 °C)
TM1P	−0.0143	−0.0071	TM2P	−0.0159	−0.0077

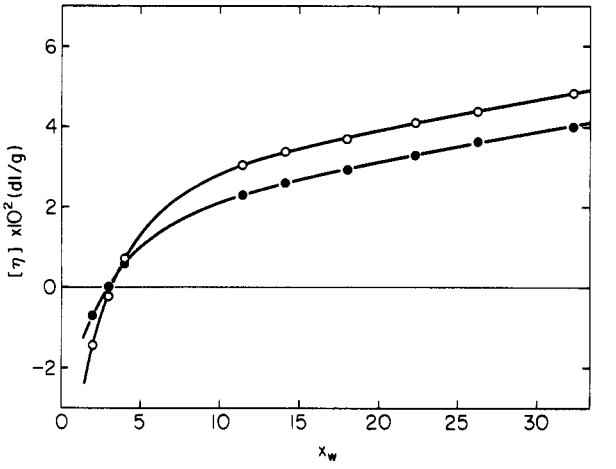

Figure 5. Plots of $[\eta]$ against x_w for OIB samples. (○) In IAIV at 25.0 °C; (●) in benzene at 25.0 °C.

Thus, it is convenient and necessary to plot the values of $[\eta]$ themselves against M_w or the weight-average degree of polymerization, x_w, in the oligomer region. Figure 5 shows such plots for OIB2–OIB32, the symbols having the same meaning as in Figure 4. The values of $[\eta]$ are definitely larger in IAIV than in benzene, with the difference being almost independent of x_w for $x_w \gtrsim 10$. However, the difference becomes small as x_w is decreased from ca. 10, then the relation reverses at x_w between 3 and 4, and finally $[\eta]$ drops below zero. In any case, the overall behavior in the oligomer region is similar to that for *n*-alkanes in benzene.[13]

Discussion

Effects of Specific Interactions. We have found that although $[\eta]$ of PIB has the same values in the two Θ solvents for large M_w, it becomes appreciably dependent on solvent as M_w is decreased, and moreover, it becomes negative in the lowest oligomer region. As mentioned in the Introduction section, this "anomalous" behavior may be regarded as arising from specific interactions between polymer and solvent molecules and can never be treated molecular-theoretically within the framework of classical hydrodynamics. Thus, we first consider the problem of removing such effects in order to determine the HW model parameters from a comparison of the data with our classical transport theory of $[\eta]$.

Consider the HW touched-bead model composed of N identical spherical beads of diameter d_b whose centers are located on the HW chain contour of total length $L = Nd_b$. The classical hydrodynamic theoretical value of its intrinsic viscosity, which we designate by $[\eta]_C$, may be given as a sum of the solution $[\eta]_{KR}$ of the Kirkwood–Riseman equation and the Einstein intrinsic viscosity $[\eta]_E$ of the

single bead,[17]

$$[\eta]_C = [\eta]_{KR} + [\eta]_E \quad (1)$$

with

$$[\eta]_E = 5\pi N_A d_b^3/12M_b \quad (2)$$

where N_A is Avogadro's number and M_b ($=M/N$) is the molecular weight of the bead. We note that eq 1 is valid in the approximation that we neglect terms of $\mathcal{O}(R^{-2})$ in the expansion of the Oseen tensor $\mathbf{T}(\mathbf{R}+\mathbf{r})$ around $\mathbf{r}=0$ (with $\mathbf{R}$ being the vector distance between beads),[25,26] although the equivalent form has been used earlier without derivation.[27,28] In the present case, it is clear that eq 1 as it stands may be used in the range of large M where the observed $[\eta]$ is independent of solvent. For smaller M, however, we must introduce an additional (negative) term representing the effects of specific interactions and write $[\eta]$ as

$$[\eta] = [\eta]_C + \eta^* \qquad (\eta^* \le 0) \quad (3)$$

If we assume that this modification applies only to the term $[\eta]_E$ (not to $[\eta]_{KR}$), following Fixman,[26] then η^* must be independent of M, so that

$$\lim_{M\to\infty} ([\eta]/[\eta]_C) = 1 \quad (4)$$

Now let the subscripts (1) and (2) indicate solvents IAIV and benzene, respectively. As noted above, the difference $[\eta]_{(1)} - [\eta]_{(2)}$ at a given M_w, which we designate by $\Delta\eta$, is nearly independent of M_w for $M_w \gtrsim 650$. Further, in the present case, at large M_w where the relative contribution of η^* is negligibly small, $[\eta]_C$ itself may be regarded as independent of solvent, and this is assumed to be the case for smaller M_w. Then we have

$$\Delta\eta \equiv [\eta]_{(1)} - [\eta]_{(2)} = \eta^*_{(1)} - \eta^*_{(2)} \quad (5)$$

Equations 3 and 5 are the basic equations for an analysis of the present experimental data at least for $M_w \gtrsim 650$. The problem is to determine the empirical parameter, η^*, along with the HW model parameters, including d_b, from a comparison between theory and experiment. We then note that $\Delta\eta$ is found to be 0.0078 dL/g as an average value for the six samples OIB11–OIB32.

HW Model Parameters. Now $[\eta]_C$ may be written in the form

$$[\eta]_C = (1/\lambda^2 M_L) f_\eta(\lambda L; \lambda^{-1}\kappa_0, \lambda^{-1}\tau_0, \lambda d_b) \quad (6)$$

where κ_0 and τ_0 are the differential geometrical curvature and torsion, respectively, of the characteristic helix, which the HW chain contour takes at the minimum zero of its total elastic energy, λ^{-1} is the static stiffness parameter as defined as the bending force constant divided by $k_BT/2$ with k_B being the Boltzmann constant and T being the absolute temperature, and M_L ($=M/L$) is the shift factor as defined as the molecular weight per unit contour length. The function f_η is defined by

$$f_\eta(\lambda L) = \lambda^{-1} M_L [\tilde{\eta}]_C \quad (7)$$

where $[\tilde{\eta}]_C$ is the $[\eta]_C$ measured in units of $(\lambda^{-1})^3$ and is given by eq 15 with eqs 17 and 27 of ref 17. It satisfies the following asymptotic relation

$$\lim_{\lambda L\to\infty} f_\eta(\lambda L)/(\lambda L)^{1/2} = c_\infty^{3/2}\Phi_\infty \quad (8)$$

Table IV
Values of the HW Model Parameters from $[\eta]$

polymer (f_r)	solvent	temp, °C	$\lambda^{-1}\kappa_0$	$\lambda^{-1}\tau_0$	λ^{-1}, Å	M_L, Å^{-1}	d_b, Å
PIB	IAIV, benzene	25.0	0		12.7	24.1	6.4
a-PS (0.59)	cyclohexane	34.5	3.0	6.0	23.5	42.6	10.1
a-PMMA (0.79)	acetonitrile	44.0	4.5	2.0	45.0	38.6	7.2

with

$$c_\infty = \frac{4 + (\lambda^{-1}\tau_0)^2}{4 + (\lambda^{-1}\kappa_0)^2 + (\lambda^{-1}\tau_0)^2} \quad (9)$$

and with Φ_∞ ($=2.870\times10^{23}$ mol^{-1}) being the coil limiting value of Φ.

As mentioned in the Introduction section, it is impossible to determine all five of the model parameters, κ_0, τ_0, λ^{-1}, M_L, and d_b, involved in $[\eta]_C$ together with η^*, since the double-logarithmic plots of $[\eta]$ against M_w deviate only slightly from the straight line of slope $^1/_2$ except in the oligomer region, as seen from Figure 4. Fortunately, however, it is known that the PIB chain takes a form close to the 8_3 helix of pitch 18.60 Å in the crystalline state,[29] and we assume that this conformation is locally preserved also in dilute solutions. The PIB chain is then very symmetric about its helix axis, and we may represent it by the KP wormlike chain, taking the helix axis as the contour of the latter, as in the case of poly(*n*-alkyl isocyanate)s.[30,31] Since the KP chain is a special case of the HW chain with $\kappa_0 = 0$, eq 9 then reduces to

$$c_\infty = 1 \qquad \text{(KP)} \quad (10)$$

Thus, from eq 6, we have as the basic equations for an analysis of the data

$$\log [\eta]_C = \log f_\eta(\lambda L; \lambda d_b) - \log(\lambda^2 M_L) \quad (11)$$

$$\log M = \log(\lambda L) + \log(\lambda^{-1} M_L) \quad (12)$$

In principle, the quantities $\lambda^2 M_L$ and $\lambda^{-1}M_L$ may then be estimated from a best fit of the double-logarithmic plots of the theoretical f_η against λL for properly chosen values of λd_b to those of the "observed" $[\eta]_C = [\eta] - \eta^*$ against M_w with properly chosen η^*, so that we may determine λ^{-1}, M_L, d_b, and η^*. However, because of the behavior of the data mentioned above, it is still difficult to determine unambiguously all of them. Thus, by using the observed asymptotic value of $[\eta]/M_w^{1/2}$ and assigning M_L the value 24.1 Å^{-1} corresponding to the above 8_3 helix from the start, we determine λ^{-1} from

$$\lim_{M\to\infty} [\eta]/M^{1/2} = \Phi_\infty(\lambda M_L)^{-3/2} \quad (13)$$

Note that this equation has been obtained from eqs 4, 6, 8, and 10. It is then rather easy to determine the remaining parameters d_b and η^* following the above procedure, where η^* must satisfy eq 5 with $\Delta\eta = 0.0078$ dL/g. The values of the parameters thus determined are given in the first row of Table IV.

Figure 6 shows double-logarithmic plots of $[\eta] - \eta^*$ ($=[\eta]_C$) against M_w for PIB. The unfilled and filled circles represent the experimental values in IAIV with $\eta^* = 0$ and in benzene with $\eta^* = -0.0078$ dL/g, respectively, both at 25.0 °C (Θ). The solid curve represents the best-fit theoretical values for $N \ge 2$ calculated from eqs 11 and 12 with the above model parameters in Table IV, the dashed line segment connecting those values for $N = 1$ and 2. The dotted line indicates the asymptotic straight

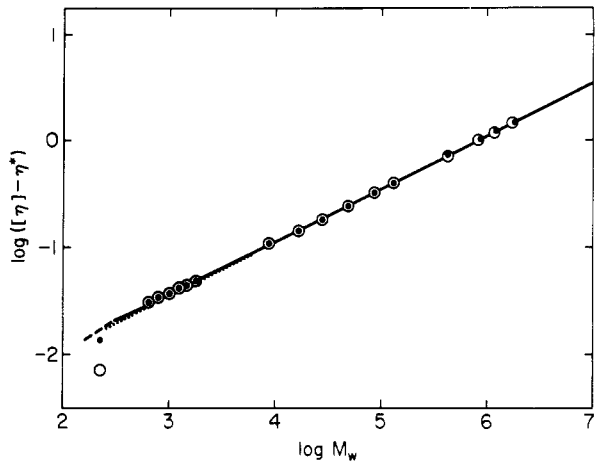

Figure 6. Double-logarithmic plots of $[\eta] - \eta^*$ (in dL/g) against M_w for PIB. (○) In IAIV at 25.0 °C ($\eta^* = 0$); (●) in benzene at 25.0 °C ($\eta^* = -0.0078$ dL/g). The solid curve represents the best-fit HW theoretical values for $N \geq 2$, the dashed line segment connecting the values for $N = 1$ and 2. The dotted straight line has a slope of 0.5.

line of slope $^1/_2$. It is seen that the agreement between theory and experiment is very good for $M_w \gtrsim 600$, and that three successive repeating units or so correspond to the single bead. Even with the new parameter η^*, the theory cannot completely explain the behavior of $[\eta]$ in the oligomer region (OIB2–OIB4), the dimer (OIB2) being beyond the range of its applicability. As for the trimer and tetramer, the disagreement between theory and experiment may probably be due to significant end effects.

In Table IV are also given the values of the model parameters determined from $[\eta]$ for a-PS ($f_r = 0.59$)[2] and a-PMMA ($f_r = 0.79$),[6] for comparison. It is seen that the PIB chain has a much smaller λ^{-1} than these asymmetric chains; in other words, the former is much more flexible. The diameter (d_b) of the PIB chain is also small compared to those of the other two. However, the result seems reasonable since it is rather consistent with the assumed local chain conformation, i.e., the 8_3 helix. The indication is that this assumption is justified. We note that, without the parameter η^*, the diameter of PIB in benzene is estimated to be unreasonably small.

Concluding Remarks

We have been able to determine the HW model parameters for PIB from the analysis of the data for $[\eta]$ in the Θ solvents, in which systems there may be specific interactions, with the introduction of the new empirical parameter η^* representing such effects at least in the range of $M_w \gtrsim 650$ where η^* (or the difference $\Delta\eta$) is independent of M_w. Unfortunately, we have failed to determine the precise range of application of this procedure in the present systems since there are no data in the range of M_w from 224 to 641 (OIB4–OIB11). In this connection, it must be noted that it is very difficult to obtain a large enough amount of original OIB sample in this range by living cationic polymerization.

A phenomenological interpretation of the negative intrinsic viscosity itself for binary simple liquid mixtures, including oligomer solutions, has already been given by, for instance, Bloomfield and Dewan.[32] Recently, Fixman[26] has also attempted to interpret it within the framework of classical hydrodynamics with a consideration of internal deformability of oligomers. At any rate, however, a complete molecular-theoretical interpretation of the negative intrinsic viscosity or the parameter η^* is one of the future problems.

Our final remark is concerned with the relation to the high-frequency dynamic intrinsic viscosity $[\eta']_\infty$, which has been found to be negative or positive.[33] It is clear that the negative intrinsic viscosity or η^* is definitely related to the negative $[\eta']_\infty$. However, it is not certain whether we should introduce the positive parameter η^* when $[\eta']_\infty$ is positive. Even so, positive η^* cannot be determined unambiguously from experiment. If the term η^* is suppressed in that case, the diameter d_b may be somewhat overestimated, but then the effect cannot be distinguished from solvation. This is the reason why we confine ourselves to the case of negative η^*.

Acknowledgment. We have benefitted from numerous suggestions given by Dr. M. Sawamoto of our department concerning the preparation and structure of isobutylene oligomers and also thank Dr. Y. Hirokawa of Nippon Zeon Co. for his preparation of the original samples OIBII and OIBIII by living cationic polymerization. This research was supported in part by a Grant-in-Aid (01430018) from the Ministry of Education, Science, and Culture, Japan.

References and Notes

(1) Konishi, T.; Yoshizaki, T.; Shimada, J.; Yamakawa, H. *Macromolecules* **1989**, *22*, 1921.
(2) Einaga, Y.; Koyama, H.; Konishi, T.; Yamakawa, H. *Macromolecules* **1989**, *22*, 3419.
(3) Konishi, T.; Yoshizaki, T.; Saito, T.; Einaga, Y.; Yamakawa, H. *Macromolecules* **1990**, *23*, 290.
(4) Koyama, H.; Yoshizaki, T.; Einaga, Y.; Hayashi, H.; Yamakawa, H. *Macromolecules* **1991**, *24*, 932.
(5) Tamai, Y.; Konishi, T.; Einaga, Y.; Fujii, M.; Yamakawa, H. *Macromolecules* **1990**, *23*, 4067.
(6) Fujii, Y.; Tamai, Y.; Konishi, T.; Yamakawa, H. *Macromolecules* **1991**, *24*, 1608.
(7) Yamakawa, H. *Annu. Rev. Phys. Chem.* **1984**, *35*, 23.
(8) Yamakawa, H. In *Molecular Conformation and Dynamics of Macromolecules in Condensed Systems*; Nagasawa, M., Ed.; Elsevier: Amsterdam, 1988; p 21.
(9) Konishi, T.; Yoshizaki, T.; Yamakawa, H. *Polym. J.* **1988**, *20*, 175.
(10) Konishi, T.; Tamai, Y.; Fujii, M.; Einaga, Y.; Yamakawa, H. *Polym. J.* **1989**, *21*, 329.
(11) Fox, T. G; Flory, P. J. *J. Phys. Colloid Chem.* **1949**, *53*, 197; *J. Am. Chem. Soc.* **1951**, *73*, 1909.
(12) Kratky, O.; Porod, G. *Recl. Trav. Chim.* **1949**, *68*, 1106.
(13) Rempp, P. *J. Polym. Sci.* **1957**, *23*, 83.
(14) von Meerwall, E. D.; Amelar, S.; Smeltzly, M. A.; Lodge, T. P. *Macromolecules* **1989**, *22*, 295.
(15) Dunstan, A. E. *J. Chem. Soc. London* **1904**, *85*, 817.
(16) Herz, von W.; Rathmann, W. *Z. Elektrochem.* **1913**, *19*, 589.
(17) Yoshizaki, T.; Nitta, I.; Yamakawa, H. *Macromolecules* **1988**, *21*, 165.
(18) Kennedy, J. P. *Cationic Polymerization of Olefins: A Critical Inventory*; Wiley-Interscience: New York, 1975.
(19) Kennedy, J. P.; Chang, V. S. C.; Smith, R. A.; Ivan, B. *Polym. Bull.* **1979**, *1*, 575.
(20) Rubingh, D. N.; Yu, H. *Macromolecules* **1976**, *9*, 681.
(21) Berry, G. C. *J. Chem. Phys.* **1966**, *44*, 4550.
(22) Krigbaum, W. R.; Flory, P. J. *J. Am. Chem. Soc.* **1953**, *75*, 5254.
(23) Kaszas, G.; Puskas, J. E.; Chen, C. C.; Kennedy, J. P. *Polym. Bull.* **1988**, *20*, 413.
(24) Matsumoto, T.; Nishioka, N.; Fujita, H. *J. Polym. Sci., A-2* **1972**, *10*, 23.
(25) Yoshizaki, T.; Yamakawa, H. *J. Chem. Phys.* **1988**, *88*, 1313.
(26) Fixman, M. *J. Chem. Phys.* **1990**, *92*, 6858.
(27) Bianchi, U.; Peterlin, A. *J. Polym. Sci., A-2* **1968**, *6*, 1759.
(28) Dewan, R. K.; Bloomfield, V. A.; Berget, P. B. *J. Phys. Chem.* **1971**, *75*, 3120.
(29) Kusanagi, H.; Tadokoro, H.; Chatani, Y. *Polym. J.* **1977**, *9*, 181.
(30) Yamakawa, H.; Shimada, J.; Nagasaka, K. *J. Chem. Phys.* **1979**, *71*, 3573.
(31) Murakami, H.; Norisuye, T.; Fujita, H. *Macromolecules* **1980**, *13*, 345.
(32) Bloomfield, V. A.; Dewan, R. K. *J. Phys. Chem.* **1971**, *75*, 3113 and references cited therein.
(33) Morris, R. L.; Amelar, S.; Lodge, T. P. *J. Chem. Phys.* **1988**, *89*, 6523.